Intramolecular carbonyl-ene reaction of citronellal to isopulegol over ZnBr$_2$-loading mesoporous silica catalysts

Shohei Imachi [1], Kisho Owada, Makoto Onaka *

Department of Chemistry, Graduate School of Arts and Science, The University of Tokyo, Meguro, Tokyo 153-8902, Japan

Abstract

We report the preparation of ZnBr$_2$-loading mesoporous catalysts and their application to the intramolecular carbonyl-ene reaction of (+)-citronellal to (−)-isopulegol. The mesoporous catalysts were characterized by N$_2$ adsorption–desorption isotherms, X-ray powder diffraction (XRD), scanning electron microscopy (SEM), and inductively coupled plasma atomic emission spectrometry (ICP-AES). Among a series of mesoporous supports, C8-HMS, which was synthesized from Si(OEt)$_4$ via a sol–gel process in the presence of octylamine as a templating agent, was found to be an optimal support to load ZnBr$_2$ without damage of inherent mesoporosity of the support. The ZnBr$_2$ loaded on C8-HMS (ZnBr$_2$/C8-HMS) showed higher catalytic activity and diastereoselectivity than ZnBr$_2$ on other HMS with different particle and pore sizes, MCM-41, mesoporous alumina, and Al-HMS. The amount of zinc ions eluted into the solution phase from ZnBr$_2$/C8-HMS was only at a less than 1 ppm level. The results suggested that clumped ZnBr$_2$ was no longer formed on the mesoporous silica surface. The ZnBr$_2$/C8-HMS catalyst which had been washed well with excess EtOH still contained zinc species, but had neither catalytic activity nor bromide ions. It was concluded that at least two different kinds of Zn sites existed on the surface of ZnBr$_2$/C8-HMS; one site was the crystallite ZnBr$_2$ which was finely dispersed on the silica surface, and the other was oxygenated zinc species such as Zn(OSi≡)$_2$ and/or Zn(OH)(OSi≡).

1. Introduction

As the skeleton of a menthol molecule has three stereogenic centers, eight diastereomers are possible. However, among the isomers (−)-menthol is only one beneficial isomer as an ingredient for cigarettes, chewing gums, toothpastes, pharmaceutical and personal-care products [1], and 4500 t a year of the compound is consumed worldwide. In the current menthol industry, (−)-menthol is mainly provided by three routes [2]: (1) extraction from natural mint in China and Brazil; (2) synthesis of racemic menthol from *m*-cresol via the formation of thymol (2-isopropyl-5-methylphenol) and its reduction with hydrogen, followed by optical resolution; (3) chemical synthesis from myrcene through asymmetric isomerization of diethylgeranylamine with an Rh-BINAP catalyst and an intramolecular carbonyl-ene reaction as key steps (the Takasago process) [3].

In the Takasago process, myrcene, produced by thermal cracking of β-pinene, reacts with diethylamine in the presence of a catalyst of *n*-BuLi to give diethylgeranylamine stereoselectively. Asymmetric isomerization of diehtylgeranylamine to citronellal (*R,E*)-diethylamine by a chiral rhodium/(*S*)-BINAP catalyst is the most remarkable step in the Takasago process. Additionally, we should consider another step of intramolecular cyclization of (*R*)-(+)-citronellal to (−)-isopulegol an equally important stage, because the cyclization of citronellal can afford four diastereoisomers, among which (−)-isopulegol is only a desirable precursor to (−)-menthol.

In the Takasago process, isomerization of (+)-citronellal to (−)-isopulegol, which is classified as an intramolecular carbonyl-ene reaction, was originally performed in up to 92% diastereoselectivity in the presence of ZnBr$_2$, which had been discovered by Nakatani and Kawashima [4]. However, there were some shortcomings that the reaction requires a stoichiometric amount of solid ZnBr$_2$, some of which were dissolved in organic solvents such as CH$_2$Cl$_2$ and benzene. Recently Takasago patented a new homogeneous catalyst of tris(2,6-diarylphenyloxy)aluminum for the cyclization of (+)-citronellal

[5]. Although this catalyst promotes the cyclization in over 95% yield of (−)-isopulegol with almost 100% diastereoselectivity, the catalyst is difficult to be separated from the reaction mixture and to be reused. Therefore, discovering a new heterogeneous catalyst system has been paid much attention to by many chemists, and several heterogeneous catalysts for the cyclization have been reported.

Corma et al. reported that water-tolerant and Lewis acidic Sn-β zeolite in which tin ions were isomorphically substituted into the β zeolite framework worked as an efficient catalyst for the cyclization of (+)-citronellal [6]. The catalyst recorded a turnover number of 1350 per tin ion in 83% diastereoselectivity without elution of tin ions.

Zirconium ion-exchanged montmorillonite was also an excellent solid catalyst for the cyclization with 90% selectivity, and was able to be reused at least five times with the same activities [7]. Zr-β zeolite, which was synthesized by the incorporation of zirconium ions into β zeolite, also showed high diastereoselectivity [8].

Typical porous silica-based catalysts accelerated the cyclization of (+)-citronellal as well: the cyclization was drastically improved by using H_3PO_4- or heteropolyacid-loading silica gel, while both catalysts showed only moderate diastereoselectivities [9,10]. Galvagno et al. prepared Zn(II)-loading catalysts by impregnation of amorphous silica with a solution of $ZnBr_2$, followed by drying, and the catalysts were found to show up to 86% diastereoselectivity [11,12]. According to their investigation, the silica surface consists of both physically adsorbed $ZnBr_2$ and Zn(II) sites of zinc oxy-hydroxide and/or $Zn(OSi\equiv)_2$. The Zn(II) sites are the most active for the cyclization, but the physically adsorbed $ZnBr_2$ is required to attain high diastereoselectivity. In other words, the $ZnBr_2$ site was less active but more diastereoselective than the Zn(II) sites. Then, it is easy to envisage that more active and higher diastereoselective catalysts can be realized if support materials are covered with well-dispersed $ZnBr_2$ salts on the surface.

In recent years, a lot of mesoporous materials have been developed such as silica, aluminosilicate, and alumina. Generally, mesoporous materials which have uniform mesopores and high specific surface areas are prepared in the presence of proper template agents through a sol–gel process. Compared with the use of amorphous or microporous supports, that of mesoporous supports provides us several remarkable advantages: (1) the nano-sized uniform pore structure prevents $ZnBr_2$ crystal from agglomerating, (2) the large surface area enables the support to hold a large amount of active species on the surface, and (3) the size of mesopore is large enough to diffuse a variety of organic substrates and products smoothly.

To make the best use of these features leads to the preparation of various effective catalysts. For example, we have already reported that MoO_3 supported on HMS showed remarkable catalysis for olefin metathesis against MoO_3 on normal silica [13]. It was also demonstrated that Re_2O_7 finely dispersed on mesoporous alumina more effectively catalyzed the metathesis of terminal and inner olefins than Re_2O_7 on γ-alumina [14]. More recently, we discovered that methyltrioxorhenium on $ZnCl_2$-modified mesoporous alumina catalyzed the metathe-
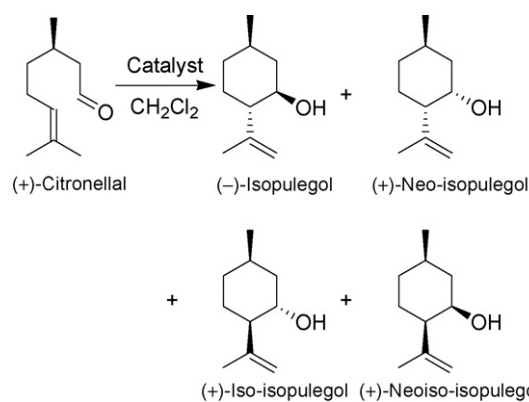

Fig. 1. Four diastereoisomers from the cyclization of (+)-citronellal.

sis not only of simple olefins but also of olefins functionalized with ester, carbonyl, and halogen groups [15].

This article describes the preparation and characterization of $ZnBr_2$ loading mesoporous catalysts in detail and their application for the cyclization of (+)-citronellal to (−)-isopuregol in a high diastereoselective way (Fig. 1).

2. Experimental

2.1. General

Commercially available (+)-citronellal (Tokyo Kasei Kogyo) was distilled before use. CH_2Cl_2, EtOH and CH_3CN (Kanto Chemical) were dried over Molecular Sieves 4A. SiO_2 (Fuji Silysia Chemical, CARiACT Q-3), $Si(OEt)_4$ (Tokyo Kasei Kogyo), colloidal silica (Aldrich, HS-40, 40 wt% suspension in water), *n*-octylamine (Tokyo Kasei Kogyo), *n*-dodecylamine (Tokyo Kasei Kogyo), *n*-hexadecylamine (Kanto Chemical), *n*-hexadecyltrimethylammonium chloride (Kanto Chemical), Al(O-*s*-Bu)$_3$ (Tokyo Kasei Kogyo), NH_4OH (Kanto Chemical, 30 wt%), 1-propanol (Kanto Chemical), lauric acid (Kanto Chemical), Al(O-*i*-Pr)$_3$ (Kanto Chemical) and $ZnBr_2$ (Kanto Chemical) were used without further purification. Infrared (IR) spectra were recorded on a JASCO FT550 FT-IR spectrometer. ^{1}H NMR spectra were recorded on a JEOL JNM-GSX270 (270 MHz) or a JEOL JNM-GSX500 (500 MHz) spectrometer; chemical shifts (δ) are reported in parts per million relative to tetramethylsilane. Splitting patterns are designed as s, singlet; d, doublet; t, triplet; q, quartet; m, multiplet; br, broad. ^{13}C NMR spectra were recorded on a JEOL EX270 (68 MHz) spectrometer with complete proton decoupling. Chemical shifts were recorded in parts per million relative to tetramethylsilane with the solvent resonance as internal standard (CDCl$_3$; δ 77.0 ppm). N_2 adsorption–desorption measurements were performed at −196 °C with a Belsorp 28SA (Bel Japan, Inc.) using static adsorption procedures. Samples were outgassed at 400 °C and 1.3 Pa for 12 h prior to analysis. Specific surface area (S.A.) was determined by the BET method. Pore diameter (P.D.) was calculated by means of the BJH method. Gas chromatography analysis (GC) was carried out with a Shimadzu GC-8A equipped with an FID detector and a 25 m OV-1 chemically bonded capillary column. X-ray powder diffraction

(XRD) patterns were recorded on a Rigaku MULTI FLEX. Inductively coupled plasma atomic emission spectrometry (ICP-AES) was recorded on a Rigaku SPECTROCIROS CCD. Scanning electron microscopy (SEM) was run using a Keyence VE-9800 operated at 3 kV without carbon coating treatment.

2.2. Synthesis of mesoporous materials

2.2.1. HMS (C8-HMS)

Under vigorous stirring, $Si(OEt)_4$ (100 mmol) was added to a mixture of EtOH (650 mmol), deionized water (3 mol) and *n*-octylamine (25 mmol). The resulting mixture was aged by stirring for 48 h at room temperature. Then, the resulting gel was filtered, washed with EtOH, dried in vacuo at 120 °C. The solid material was heated to 600 °C at a ramping rate of 5 °C/min in an N_2 flow, and calcined at 600 °C in air for 4 h. When *n*-dodecylamine and *n*-hexadecylamine for the synthesis of C12- and C16-HMS were used as templating agents, the molar compositions of $Si(OEt)_4$:amine:EtOH:H_2O were 1.0:0.25:8.5:28.4 and 1.0:0.3:14:23, respectively.

2.2.2. MCM-41

Thirty-weight percentage of NH_4OH (0.49 g) was added to a solution of *n*-hexadecyltrimethylammonium chloride (29 mmol) and deionized water (1.45 mol), and the mixture was stirred for 1 h at ambient temperature. The resulting solution was mixed with a solution of colloidal silica (34.3 g) and aqueous NaOH (1 M, 105 g), and the mixture was stirred for 1 h at ambient temperature. The reaction mixture was put into an oven and kept statically for 4 days at 110 °C. Under the heating, pH of the solution was checked every 24 h and adjusted with acetic acid to 11.0. The resulting solid was filtered, washed with deionized water, dried under an N_2 flow over 12 h. The dried solid was then heated to 500 °C at a ramping rate of 5 °C/min in an N_2 flow, and calcined at 500 °C in air for 5 h.

2.2.3. meso-Al2O3

In a 500 ml polypropylene bottle a mixture of $Al(O\text{-}s\text{-}Bu)_3$ (178 mmol) and 1-propanol (6 mol) was stirred for 10 min, and then deionized water (572 mmol) was added. The solution was stirred for 60 min at room temperature, followed by addition of a solution of lauric acid (54 mmol) in 1-propanol (580 mmol). The mixture was stirred for 24 h at room temperature, and then transferred into a 300 ml autoclave. The mixture was aged at 110 °C for 48 h without stirring. After filtration, the white solid was washed with EtOH (100 ml), and dried under an N_2 flow overnight at room temperature. The solid material was heated to 600 °C at a ramping rate of 1 °C/min in air flow, and calcined at 600 °C in air for 4 h.

2.2.4. Al-HMS (Si/Al = 6.8)

To a vigorously stirred solution of $n\text{-}C_{16}H_{33}NH_2$ (3.31 mmol) in EtOH (153 mmol) and deionized water (257 mmol) was added at a time a homogeneous mixture of $Si(OEt)_4$ (10 mmol) and $Al(O\text{-}i\text{-}Pr)_3$ (143 mmol) at room temperature. The mixture was vigorously stirred for 48 h at room temperature. The white gel formed was collected and dried at room temperature under an N_2

flow. The dried gel was set in an electric furnace, and gradually heated to 500 °C for 5 h in dry air.

2.3. Synthesis of ZnBr2-loading catalyst

A typical procedure was described for the preparation of $ZnBr_2$/C8-HMS: an EtOH (20 ml) solution of $ZnBr_2$ (4.0 mmol) was added to powder C8-HMS (8.46 g), and the mixture was dried under an N_2 flow until EtOH was dried up. Then, the following procedure was repeated twice: EtOH (20 ml) was added to the sapless solid, and the mixture was stirred slowly for 1 min, followed by being dried again in an N_2 flow. The $ZnBr_2$-loading HMS was heated to 400 °C at a ramping rate of 7 °C/min in an N_2 flow, and calcined at 400 °C in air for 4 h.

2.4. Cyclization of (+)-citronellal to (−)-isopulegol

To $ZnBr_2$/C8-HMS (activated at 400 °C under below 133 Pa for 4 h) containing 0.1 mmol of $ZnBr_2$ was added a CH_2Cl_2 solution (10 mL) of (+)-citronellal (1.0 mmol) at room temperature. After the reaction was completed, the mixture was filtrated and the filtrate was evaporated. The crude products were purified by distillation with a Kugelrohr apparatus to afford a mixture of (−)-isopulegol and other two diastereoisomers. Diastereoselectivities of (−)-isopulegol to the other diastereoisomers were determined by GC analysis using an OV-1 capillary column at 80 °C [16]—retention time: (−)-isopulegol 9.63 min, (+)-neo-isopulegol 1.08 min, (+)-*iso*-isopulegol 10.59 min. (−)-Isopulegol: ^1H NMR (500 MHz, $CDCl_3$) δ 0.92–1.01 (m, 5H), 1.30–1.36 (m, 1H), 1.48–1.51 (m, 1H), 1.66–1.71 (m, 5H), 1.90 (dt, $J = 1.6$ and 9.8 Hz, 1H), 1.96 (m, 1H), 2.03–2.05 (m, 1H), 3.46 (dt, $J = 4.3$ and 10.5 Hz, 1H), 4.87 (d, $J = 2.8$ Hz, 2H). ^{13}C NMR ($CDCl_3$) δ 18.1, 22.0, 24.5, 31.2, 34.1, 42.5, 53.8, 70.2, 112.5, 146.4.

3. Results and discussion

3.1. Application of mesoporous materials and zinc salt-loading ones for the cyclization of citronellal

In the present study, we selected several mesoporous materials of silica (HMS [17,18] and MCM-41 [19]), alumina (*meso*-Al_2O_3 [20]) and aluminosilicate (Al-HMS [21]). Silica gel (SiO_2) was also used as a control. Especially, we prepared three types of HMS with different pore sizes using varied alkylamine templates with C8, C12, and C16 carbon chains, and abbreviate them to C*n*-HMS (*n* = 8, 12, and 16). Physical properties of the materials are summarized in Table 1.

First we applied the mesoporous materials as solid catalysts to the cyclization of (+)-citronellal to (−)-isopulegol as shown in Table 1. Although C16-HMS has almost the same surface area and pore diameter as MCM-41, these materials had different mesoporous structures: HMS possesses wormhole-like mesopores, thicker walls, more cross-linked silica framework and smaller particle sizes, while MCM-41 has a hexagonally arranged, long tunnel mesoporous structure.

Table 1
Mesoporous material catalyzed cyclization of citronellal[a]

Entry	Catalyst	S.A. ($m^2\,g^{-1}$)	P.D. (nm)	Time (h)	Yield (%)	Selectivity[b] (%)
1	C16-HMS	880	2.9	18	60	75
2	MCM-41	930	2.7	18	10	–
3	SiO$_2$	700	3.6	18	40	71
4	*meso*-Al$_2$O$_3$	360	3.6	18	Trace	–
5	Al-HMS	1100	2.6	5	77	75

[a] (+)-Citronerall (1.0 mmol) reacted in CH$_2$Cl$_2$ (10 ml) in the presence of catalyst (200 mg) at room temperature.

[b] Selectivity to (−)-isopulegol out of the three diastereomers detected.

Among the four possible diastereomers ((−)-isopulegol, (+)-neo-isoplegol, (+)-*iso*-isoplegol, and (+)-neoiso-isoplegol), the most thermodynamically unstable isomer, (+)-neoiso-isoplegol, was not detected through all the experiments in the study. Interestingly, between the two mesoporous pure silicas, HMS showed much higher catalytic activity than MCM-41 (entries 1 and 2). Although the cyclization proceeded on SiO$_2$, the activity was somewhat low (entry 3). It is also interesting to find that mesoporous aluminosilicate, Al-HMS [22], gave isopulegol in moderate yield and diastereoselectivity, because such decent diastereoselectivity would not have been expected with the use of such a highly acidic aluminosilicate (entry 5). Almost no cyclization proceeded with *meso*-Al$_2$O$_3$ composed of pure alumina (entry 4).

Nakatani et al. carefully investigated the cyclization of (+)-citronellal using various zinc salts [4], and found that ZnBr$_2$ gave the best result concerning the yield and the diastereoselectivity to (−)-isopulegol. Therefore, ZnBr$_2$ was loaded on the mesoporous materials, and physical properties of the supported catalysts and their catalytic activities for the cyclization were investigated (Table 2). Compared with catalytic activity of unloaded supports in Table 1, the catalysis of ZnBr$_2$ on C16-HMS, MCM-41 and *meso*-Al$_2$O$_3$ much improved. And more interestingly, higher diastereoselectivity was realized with C16-HMS, MCM-41, SiO$_2$ and *meso*-Al$_2$O$_3$ after loading of ZnBr$_2$. On the other hands, ZnBr$_2$/Al-HMS did not improve the diastereoselectivity. We suppose that the acidity of pristine Al-HMS is high enough to show high catalytic activity even though the ZnBr$_2$ is not loaded on Al-HMS.

Various zinc salt-loading catalysts (designated as ZnX$_2$/C16-HMS) were prepared by impregnation of C16-HMS with ZnF$_2$, ZnCl$_2$, ZnBr$_2$, ZnI$_2$ and Zn(NO$_3$)$_2$, and their catalytic activity is summarized in Table 3. The order of the catalysis with ZnX$_2$/HMS was almost the same as that of catalysis with parent zinc salts [4]: among zinc halides, ZnBr$_2$/C16-HMS showed

Table 3
Effects of zinc salts loaded on C16-HMS upon the cyclization[a]

Entry	Catalyst	Time (h)	Yield (%)	Selectivity[b] (%)
1	ZnF$_2$/C16-HMS	18	23	80
2	ZnCl$_2$/C16-HMS	12	94	86
3	ZnBr$_2$/C16-HMS	6	94	87
4	ZnI$_2$/C16-HMS	18	82	86
5	Zn(NO$_3$)$_2$/C16-HMS	18	36	86

[a] (+)Citronellal (1.0 mmol) was treated with ZnX$_2$ (0.1 mmol) loading C16-HMS (Si/Zn = 16) in CH$_2$Cl$_2$ (10 ml) at room temperature.

[b] Selectivity to (−)-isopulegol out of the three diastereomers.

the best yield (94%) and the highest diastereoselectivity (87%) (entry 3), and ZnF$_2$/C16-HMS the lowest of 23% (entry 1). (−)-Isopulegol was obtained in a poor yield with ZnO loaded on HMS, which had been prepared through calcination of Zn(NO$_3$)$_2$-loading HMS in air at 400 °C (entry 5).

Although ZnBr$_2$/C16-HMS catalyst gave such a good result, it was found that C16-HMS underwent partial degradation of the mesoporosity during the loading process of ZnBr$_2$ on the surface, because the specific surface area and the pore volume of the ZnBr$_2$/C16-HMS catalyst obviously decreased as shown in Tables 1 (entry 1), and 2 (entry 1). Therefore, it seems that part of zinc bromide active for the reaction would be buried in the silica networks through the collapse, which disturbed a close contact between the zinc sites and reactants. If the loading of ZnBr$_2$ on HMS is achieved without damage of the mesoporosity, the catalytic activities would be improved. In the next section, we have searched for tougher mesoporous HMS materials.

3.2. Preparation of ZnBr$_2$ loading HMS catalyst without degradation of mesoporous structure

It was reported by Tanev and Pinnavaia that the thermal stability of HMS upon calcination in air was superior to that of

Table 2
Cyclization of citronellal catalyzed by ZnBr$_2$-loading mesoporous material[a]

Entry	Catalyst	S.A. ($m^2\,g^{-1}$)	P.D. (nm)	Time (h)	Yield (%)	Selectivity[b] (%)
1	ZnBr$_2$/C16-HMS	500	2.7	6	94	88
2	ZnBr$_2$/MCM-41	500	2.7	12	85	85
3	ZnBr$_2$/SiO$_2$	550	–	18	60	86
4	ZnBr$_2$/*meso*-Al$_2$O$_3$	240	3.4	18	85	84
5	ZnBr$_2$/Al-HMS	760	2.6	3	88	75

[a] (+)-Citronelall (1.0 mmol) reacted over ZnBr$_2$ (0.1 mmol)-loading catalyst (Si/Zn = 16 or Al/Zn = 16) in CH$_2$Cl$_2$ (10 ml) at room temperature.

[b] Selectivity of (−)-isopulegol to other diastereomers.

Table 4
Physical properties of pristine HMS and $ZnBr_2$-loading HMS

Entry	HMS and $ZnBr_2$/HMS	S.A. ($m^2 g^{-1}$)	P.D. (nm)	P.V. ($ml g^{-1}$)
1	C8-HMS	1240	1.9	0.28
2	$ZnBr_2$/C8-HMS[a]	1200	1.9	0.28
3	EtOH-washed $ZnBr_2$/C8-HMS	1190	1.9	0.27
4	C12-HMS	1160	2.2	0.27
5	$ZnBr_2$/C12-HMS[a]	720	2.2	0.16
6	EtOH-washed $ZnBr_2$/C12-HMS	700	2.2	0.16
7	C16-HMS	880	2.9	0.20
8	$ZnBr_2$/C16-HMS[a]	500	2.7	0.11
9	EtOH-washed $ZnBr_2$/C16-HMS	490	2.7	0.11
10	SiO_2	700	–	0.20
11	$ZnBr_2$/SiO_2[a]	550	–	0.11

[a] $ZnBr_2$ (0.1 mmol) was loaded on Cn-HMS or SiO_2 with the ratio of Si/Zn = 16.

MCM-41 due to a thicker wall structure and a more cross-linked silica network [17]. However, in our study the thermal stability of C16-HMS was found not satisfactorily high under calcination in the presence of $ZnBr_2$ as mentioned in the previous section.

In the present work, we used three kinds of HMS with different pore diameters and surface areas as a support. Table 4 shows the physical properties of parent C8-, C12-, and C16-HMS as well as $ZnBr_2$-loading HMS (Si/Zn = 16). Properties of SiO_2 and the $ZnBr_2$-loading one are also shown as a control. As the alkyl chain length of a primary amine surfactant in preparation of mesoporous silica gets longer from C8 to C16, the pore diameter of the obtained mesoporous silica becomes larger with a smaller specific surface area, which is in good agreement with the report by Tanev and Pinnavaia [17]. It is interesting to note that those HMS exhibit very different morphologies: SEM micrographs of pristine HMS indicate that C8-HMS consists of very small particles <200 nm in diameter (Fig. 2c), while C12-HMS and C16-HMS are larger spherical aggregates (Fig. 2b and a).

With $ZnBr_2$/C12-HMS and $ZnBr_2$/C16-HMS, the surface areas and the pore volumes drastically decreased after loading $ZnBr_2$ (Table 4, entries 4 versus 5 and 7 versus 8). After the $ZnBr_2$ loading supports were washed with EtOH, the surface areas of the resulting EtOH-washed $ZnBr_2$/Cn-HMS (n = 12 or 16) did not return to the original values (entries 5 versus 6 and 8 versus 9). The change in the HMS weight indicated that ca.70% of zinc species were extracted out from the $ZnBr_2$-loading HMS. Therefore we suppose that the decrease in the surface area of HMS upon the $ZnBr_2$ loading comes from partial collapse of the mesoporous structure of HMS during the $ZnBr_2$-loading process rather than from some blockage in mesopores with $ZnBr_2$ crystallite. Upon loading of $ZnBr_2$ on SiO_2, the surface area also decreased. In contrast, surprisingly, $ZnBr_2$/C8-HMS had almost the same surface area and pore volume as parent C8-HMS, indicating that C8-HMS was not degraded and could maintain the inherent mesostructure upon loading of $ZnBr_2$.

The destructive changes in the mesoporous structure upon the loading of $ZnBr_2$ were also confirmed by the comparison of
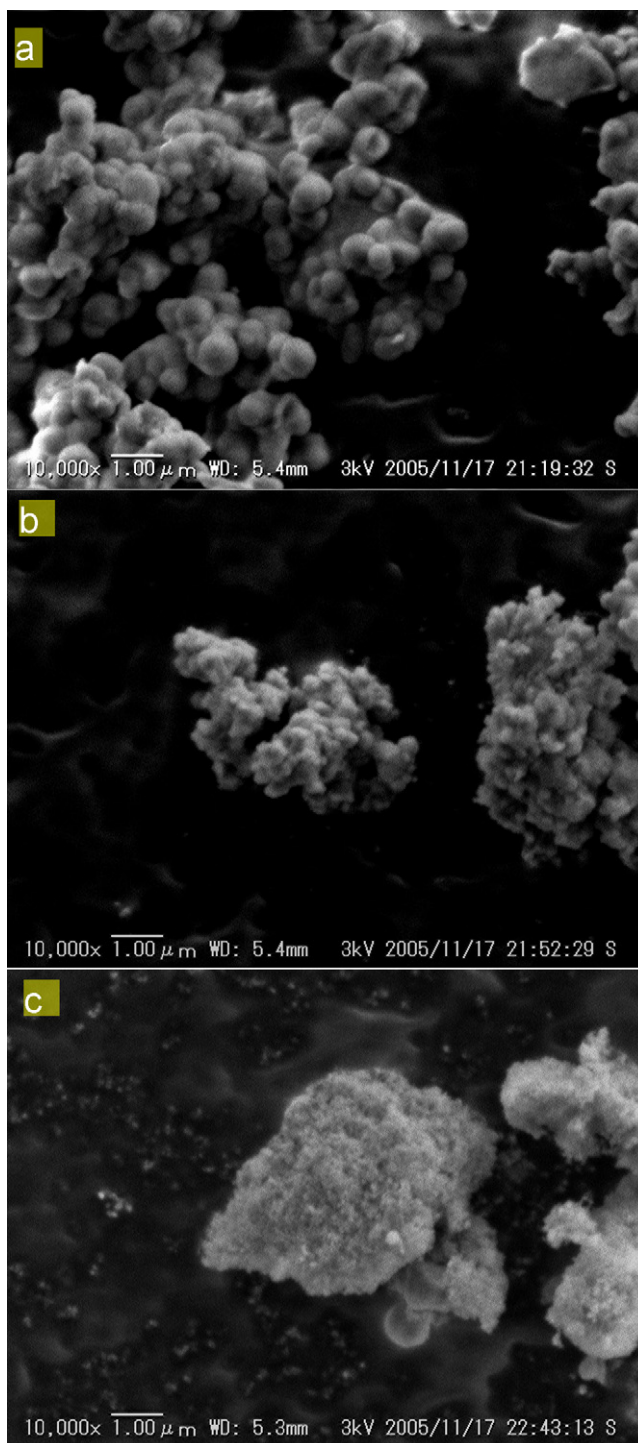

Fig. 2. SEM micrographs of (a) C16-HMS, (b) C12-HMS, and (c) C8-HMS samples. Bars indicate a scale of 1 μm.

powder XRD patterns between parent HMS and $ZnBr_2$-loading HMS, as shown in Fig. 3. Although the patterns of the parent C16-HMS and C12-HMS contained a strong [1 0 0] reflection peak at 2θ = ca. 2.5°, no reflection peaks were observable after the loading of $ZnBr_2$. In contrast, though the pattern of C8-HMS showed a very weak reflection peak, the reflection still remained after the $ZnBr_2$-loading. It can be concluded that C8-HMS with a smaller pore diameter and a particle size has an improved
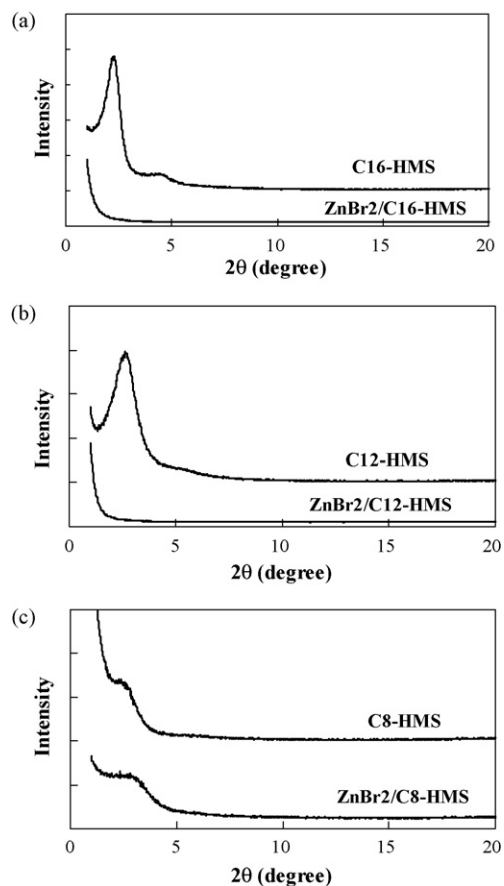
Fig. 3. Powder XRD patterns of Cn-HMS and ZnBr$_2$/Cn-HMS. (a) C16-HMS, (b) C12-HMS, and (c) C8-HMS.

thermal stability and sustains its intrinsic mesoporosity during the ZnBr$_2$-loading process.

3.3. Characterization of zinc species loaded on HMS

The elemental analysis of ZnBr$_2$-loading Cn-HMS (Si/Zn = 16) catalysts was performed with ICP-AES and is summarized in Table 5. The atomic ratios of Br/Zn of the catalysts were found to be 1.5–1.6. This result agrees with that reported by Galvagno and coworkers [11], indicating that ZnBr$_2$ was partially degraded and part of bromide ions were lost upon the loading. Interestingly, after washing ZnBr$_2$/C8-HMS with a sufficient quantity of EtOH, the C8-HMS still contained 0.8 wt% of zinc species, but almost no bromide ions remained as shown in Table 5. If ZnBr$_2$ crystallite, which had been physically adsorbed on C8-HMS and would be a real catalyst site, was washed out with excess EtOH, the residual zinc

Table 5
Elemental analysis of ZnBr$_2$/HMS catalysts

Catalyst	Zn (wt%)	Br/Zn
ZnBr$_2$/C8-HMS	2.6	1.5
ZnBr$_2$/C12-HMS	2.9	1.6
ZnBr$_2$/C16-HMS	2.8	1.5
EtOH-washed ZnBr$_2$/C8-HMS	0.8	<0.1

species on C8-HMS, which were not soluble in EtOH, would be oxy-zinc species chemically bonded to the silica framework. Actually the oxy-zinc species was found to have little catalytic activity for the cyclization of (+)-citronellal for 3 h.

We then investigated whether or not zinc species of catalyst can dissolve into a CH$_2$Cl$_2$ solution phase during the reaction: after a suspension mixture of (+)-citronellal (1.0 mmol) and zinc catalyst of bulk ZnBr$_2$ or loaded ZnBr$_2$ (0.1 mmol) in CH$_2$Cl$_2$ (10 ml) was stirred for 3 h, the reaction mixture was filtered and the filtrate was directly analyzed by ICP-AES. The bulk ZnBr$_2$ was found to be completely dissolved into 10 ml of CH$_2$Cl$_2$. If ZnBr$_2$ is loaded on C8-HMS in the form of clumps, ZnBr$_2$ should be similarly eluted into the CH$_2$Cl$_2$ solution. However, the amount of eluted zinc species from ZnBr$_2$/C8-HMS was very low on a less than 0.1% level, and in fact, the filtrate had no catalysis for the carbonyl-ene reaction. In addition, we could not observe any reflection peaks corresponding to crystalline ZnBr$_2$ on the ZnBr$_2$/C8-HMS by powder XRD. These findings lead to a conclusion that a real active site on ZnBr$_2$/C8-HMS catalyst is a crystallite of ZnBr$_2$ which is finely dispersed and well interacted with the C8-HMS surface, and that the active site shows high catalytic activity for the cyclization with excellent diastereoselectivity.

3.4. Catalytic activity of ZnBr$_2$-loading C8-HMS for the cyclization of citronellal

It is easily expected that the dispersion of active zinc sites on C8-HMS should affect the reaction rate of the cyclization. A series of ZnBr$_2$/C8-HMS catalysts with different atomic ratios of Si/Zn (i.e. varied loading amounts of ZnBr$_2$) were prepared, and their catalytic activities were compared by use of each catalyst including the same amount of ZnBr$_2$ (0.1 mmol) as summarized in Table 6. Although the diastereoselectivities were not different, the reaction period which was required for the complete consumption of citronellal was heavily influenced by the atomic ratios of Si/Zn: some unknown byproducts were produced and hence the yields of the desired products slightly decreased probably owing to the presence of more amounts of the support in the cases of entries 3 and 4. The optimal ratio Si/Zn was 32, with which the ZnBr$_2$/C8-HMS (Si/Zn = 32) catalyst showed the best result concerning the reaction rate and the chemical yield (entry 2).

In the case of Galvagno's catalyst [11], because Zn(II) sites, which were considered to be zinc oxy-hydroxide and/or Zn(O–Si≡)$_2$, were more active but less diastereoselective for the

Table 6
Effects of the atomic ratio of Si/Zn in ZnBr$_2$/C8-HMS on the reaction[a]

Entry	Si/Zn	Time (h)	Yield (%)	Selectivity[b] (%)
1	16	6	89	86
2	32	3	94	88
3	48	3	89	87
4	64	2	80	87

[a] (+)-Citronelall (1.0 mmol) reacted over ZnBr$_2$ (0.1 mmol) loading catalysts in CH$_2$Cl$_2$ (10 ml) at room temperature.
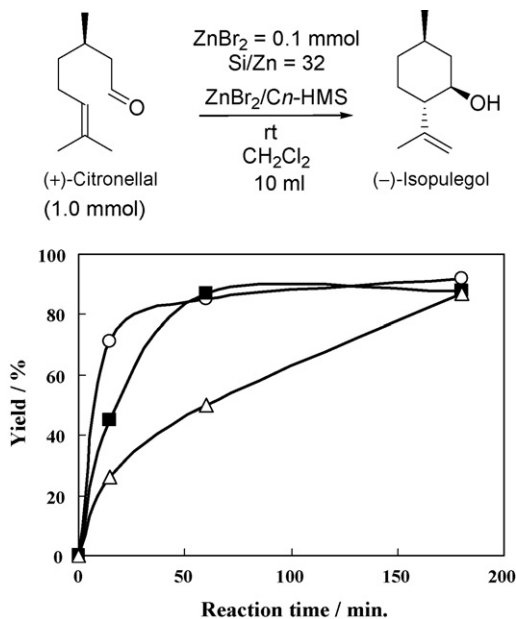[b] Selectivity to (−)-isopulegol out of the three diastereomers.

Fig. 4. Cyclization rate of citronellal over ZnBr$_2$-loading HMS catalysts. ZnBr$_2$/C16-HMS (△), ZnBr$_2$/C12-HMS (■), and ZnBr$_2$/C8-HMS (●).

Fig. 5. Cyclization of 7-methyloct-6-enal.

carbonyl-ene reaction than ZnBr$_2$ sites [12], ZnBr$_2$ had to be loaded on normal silica with a high zinc content of >4.0 mmol/g in order for ZnBr$_2$ to cloak the surface of zinc oxide species and to achieve a high diastereoselection. In contrast, although the ZnBr$_2$/C8-HMS catalyst (Si/Zn = 32) contained a much lower content (0.5 mmol/g) of ZnBr$_2$, it showed high catalytic performance and the highest diastereoselectivity to (−)-isopulegol.

The catalytic activities of ZnBr$_2$/C8-HMS, ZnBr$_2$/C12-HMS and ZnBr$_2$/C16-HMS were compared in the cyclization of (+)-citronellal as shown in Fig. 4. The cyclization rates are critically dependent on the kind of mesoporous silicas: among the three HMS catalysts, ZnBr$_2$/C8-HMS which retains the inherent mesoporosity shows the highest rate. On C-12 and C-16 HMS catalysts, some of active ZnBr$_2$ would be buried in the silica framework during the loading process of ZnBr$_2$, leading to poor catalysis.

All the catalysts were dried and activated at 400 °C under reduced pressure prior to use. Once the catalyst was used in the reaction, washing the catalyst with CH$_2$Cl$_2$ and activating it at 400 °C in vacuo were necessary for the catalyst to be reused at least twice for the cyclization in 88–94% yields with 87–88% diastereoselectivities.

3.5. Catalytic activity of ZnBr$_2$/C8-HMS for the cyclization of 7-methyloct-6-enal

The intramolecular carbonyl-ene reaction of 7-methyloct-6-enal to racemic 2-isopropenylcyclohexanol was also investigated by use of a catalytic amount of ZnBr$_2$/C8-HMS (Fig. 5). It was again proved that ZnBr$_2$ firmly loaded on C8-HMS could catalyze the cyclization at room temperature for 16 h to afford a *trans*-cyclohexanol derivative in a high yield of 90% with a high *trans/cis* selectivity of 91/9. Asymmetric cyclization of the
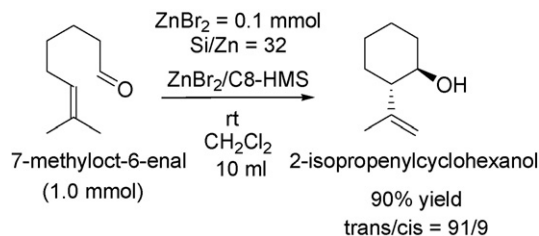
substrate has also been conducted with a combined use of titanium perchlorate and (*R*)-BINOL at room temperature for 48 h to give the products in a total yield of 66% with a *trans/cis* ratio of 69 (55% ee)/31 [23].

4. Conclusions

The present study demonstrated the preparation of ZnBr$_2$-loading mesoporous catalysts and their application to the intramolecular carbonyl-ene reaction of (+)-citronellal to (−)-isopulegol. The ZnBr$_2$-loading C8-HMS showed higher catalytic activity and diastereoselectivity than other ZnBr$_2$-loading supports such as mesoporous silicas, C12-HMS and C16-HMS, mesoporous alumina, and mesoporous aluminosilicate. The mesoporosity of mesoporous materials except for C8-HMS was partially damaged upon calcinations at high temperatures in the presence of ZnBr$_2$. Only C8-HMS could be tolerated under such harsh thermal conditions. The smaller pore diameter and smaller particle size of C8-HMS seem to be responsible for a marked improvement in the thermal stability in acidic circumstances. The preservation of uniform mesoporosity of C8-HMS enabled the ZnBr$_2$-loading catalyst to show high catalytic performance. The real catalyst site on the surface of ZnBr$_2$/C8-HMS is not oxy-zinc species directly bonded to the silica, but well-dispersed crystallite ZnBr$_2$ on the surface.

References

[1] S. Akutagawa, Organic Synthesis in Japan Past, Present and Future, Kagaku Dozin, Tokyo, 1992, pp.75–82.
[2] S. Akutagawa, Yuki Gosei Kagaku Kyokaishi 44 (1986) 513–518.
[3] K. Tani, T. Yamagata, S. Akutagawa, T. Kumobayashi, T. Taketomi, H. Takaya, A. Miyashita, R. Noyori, S. Otsuka, J. Am. Chem. Soc. 106 (1984) 5208–5217.
[4] Y. Nakatani, K. Kawashima, Synthesis (1978) 147–148.
[5] T. Iwata, Y. Okeda, Y. Hori, Eur. Pat. Appl. A2 (2002), EP1225163.
[6] A. Corma, M. Renz, Chem. Commun. (2004) 550–551.
[7] J. Tateiwa, A. Kimura, M. Tatasuka, S. Uemura, J. Chem. Soc., Perkin Trans. 1 (1997) 2169–2174.
[8] Z. Yongzhong, N. Yuntong, S. Jaenicke, G.K. Chuah, J. Catal. 229 (2005) 404–413.
[9] P.J. Kropp, G.W. Breton, S.L. Craig, S.D. Crawford, W.F. Durland Jr., J.E. Jones III, J.S. Raleigh, J. Org. Chem. 60 (1995) 4146–4152.
[10] K.A. da Silva, P.A. Robles-Dutenhefner, E.M.B. Sousa, E.F. Kozhevnikova, I.V. Kozhevnikov, E.V. Gusevskaya, Catal. Commun. 5 (2004) 425–429.
[11] C. Milone, A. Parri, A. Pistone, G. Neri, S. Galvagno, Appl. Catal. A: Gen. 233 (2002) 151–157.
[12] C. Milone, C. Gangemi, G. Neri, A. Pistone, S. Galvagno, Appl. Catal. A: Gen. 199 (2000) 239–244.

[13] T. Ookoshi, M. Onaka, Chem. Commum. (1998) 2399–2400.

[14] T. Oikawa, T. Ookoshi, T. Tanaka, T. Yamamoto, M. Onaka, Micropor. Mesopor. Mater. 74 (2004) 93–103.

[15] T. Oikawa, Y. Masui, T. Tanaka, Y. Chujo, M. Onaka, J. Organometal. Chem. 692 (2007) 554–561.

[16] P.J. Kropp, G.W. Breton, S.L. Craig, S.D. Crawford, N.F. Durland Jr., J. Org. Chem. 60 (1995) 4146–4152.

[17] P.T. Tanev, T.J. Pinnavaia, Chem. Mater. 8 (1996) 2068–2079.

[18] T.P. Pauly, Y. Liu, T.J. Pinnavaia, S.I. Billinge, T.P. Rieker, J. Am. Chem. Soc. 121 (1999) 8835–8842.

[19] J.S. Beck, J.C. Vartuli, W.J. Roth, M.E. Leonowicz, C.T. Kresge, J.B. Schmitt, C.T.-W. Chu, D.H. Olson, E.W. Sheppard, S.B. McCullen, J.B. Higgins, J.L. Schlenker, J. Am. Chem. Soc. 114 (1992) 10834–10843.

[20] F. Vaudry, S. Khodabandeh, M.E. Davis, Chem. Mater. 8 (1996) 1451–1464.

[21] P.T. Tanev, T.J. Pinnavia, Science 267 (1995) 865–867.

[22] M. Onaka, N. Hashimoto, Y. Kitabata, R. Yamasaki, Appl. Catal. A: Gen. 241 (2003) 307–317.

[23] K. Mikami, M. Terada, E. Sawa, T. Nakai, Tetrahedron Lett. 32 (1991) 6571–6574.